



Chondroitin Sulphate Proteoglycan Axonal Coats in the Human Mediodorsal Thalamic Nucleus

Harry Pantazopoulos¹, Nayeem Mubarak Hossain², Gabriele Chelini^{3,4}, Peter Durning³, Helen Barbas^{2,5,6}, Basilis Zikopoulos^{5,6} and Sabina Berretta^{3,4,7*}

¹ Department of Psychiatry and Program in Neuroscience, University of Mississippi Medical Center, Jackson, MS, United States, ² Department of Health Sciences, Boston University, Boston, MA, United States, ³ Translational Neuroscience Laboratory, Mclean Hospital, Belmont, MA, United States, ⁴ Department of Psychiatry, Harvard Medical School, Boston, MA, United States, ⁵ Department of Anatomy and Neurobiology, Boston University School of Medicine, Boston, MA, United States, ⁶ Neural Systems Laboratory, Boston University, Boston, MA, United States, ⁷ Program in Neuroscience, Harvard Medical School, Boston, MA, United States

OPEN ACCESS

Edited by:

Carmen Cavada,
Autonomous University of Madrid,
Spain

Reviewed by:

Herbert M. Geller,
National Heart, Lung, and Blood
Institute (NIH), United States
Mladen-Roko Rasin,
Rutgers, The State University
of New Jersey, United States

*Correspondence:

Sabina Berretta
s.berretta@mclean.harvard.edu

Received: 03 May 2022

Accepted: 21 June 2022

Published: 06 July 2022

Citation:

Pantazopoulos H, Hossain NM,
Chelini G, Durning P, Barbas H,
Zikopoulos B and Berretta S (2022)
Chondroitin Sulphate Proteoglycan
Axonal Coats in the Human
Mediodorsal Thalamic Nucleus.
Front. Integr. Neurosci. 16:934764.
doi: 10.3389/fnint.2022.934764

Mounting evidence supports a key involvement of the chondroitin sulfate proteoglycans (CSPGs) NG2 and brevican (BCAN) in the regulation of axonal functions, including axon guidance, fasciculation, conductance, and myelination. Prior work suggested the possibility that these functions may, at least in part, be carried out by specialized CSPG structures surrounding axons, termed axonal coats. However, their existence remains controversial. We tested the hypothesis that NG2 and BCAN, known to be associated with oligodendrocyte precursor cells, form axonal coats enveloping myelinated axons in the human brain. In tissue blocks containing the mediodorsal thalamic nucleus (MD) from healthy donors ($n = 5$), we used dual immunofluorescence, confocal microscopy, and unbiased stereology to characterize BCAN and NG2 immunoreactive (IR) axonal coats and measure the percentage of myelinated axons associated with them. In a subset of donors ($n = 3$), we used electron microscopy to analyze the spatial relationship between axons and NG2- and BCAN-IR axonal coats within the human MD. Our results show that a substantial percentage (~64%) of large and medium myelinated axons in the human MD are surrounded by NG2- and BCAN-IR axonal coats. Electron microscopy studies show NG2- and BCAN-IR axonal coats are interleaved with myelin sheets, with larger axons displaying greater association with axonal coats. These findings represent the first characterization of NG2 and BCAN axonal coats in the human brain. The large percentage of axons surrounded by CSPG coats, and the role of CSPGs in axonal guidance, fasciculation, conductance, and myelination suggest that these structures may contribute to several key axonal properties.

Keywords: axonal coat, brevican, NG2, extracellular matrix, thalamus

INTRODUCTION

In recent years, a large number of studies have demonstrated the importance of the extracellular matrix (ECM) in the regulation of developmental and adult brain processes, including synaptic plasticity and receptor trafficking (Dityatev et al., 2006; Gundelfinger et al., 2010; Frischknecht and Gundelfinger, 2012), neuronal migration (Charvet et al., 1998; Klausmeyer et al., 2011), axon

guidance (Snow et al., 2003; Kwok et al., 2012), oligodendrocyte differentiation (Ichihara-Tanaka et al., 2006; Bekku and Oohashi, 2010; Kucharova and Stallcup, 2010), and regulation of nodes of Ranvier (Bekku et al., 2009; Dours-Zimmermann et al., 2009). In addition, ECM dysregulation has been implicated in several brain disorders, including schizophrenia (Pantazopoulos et al., 2010; Consortium, 2014), bipolar disorder (Cichon et al., 2011; McGrath et al., 2013; Steullet et al., 2018), and Alzheimer's disease (Bruckner et al., 1999; Morawski et al., 2010; Yang et al., 2017).

The brain ECM surrounds all cells, occupying a volume fraction of approximately 20% of the adult brain (Thorne and Nicholson, 2006; Sykova and Nicholson, 2008). It is composed of aggregates of hyaluronan and chondroitin sulfate proteoglycans (CSPGs) connected by glycoproteins (Yamaguchi, 2000; Rauch, 2004). CSPGs consist of core proteins with varying numbers of chondroitin sulfate (CS) glycosaminoglycan chains. The chemical composition and representation of CSPGs are regulated throughout development and adulthood, modulating properties required for regulating cell migration, myelination, and axon growth (Bandtlow and Zimmermann, 2000; Wang et al., 2008; Giger et al., 2010; Maeda, 2010). In addition to a loosely organized lattice, the ECM forms highly organized structures, including pericellular ECM aggregates called perineuronal nets (PNNs), described as early as 1898 (Golgi, 1898; Celio et al., 1998). PNNs form around subsets of neurons typically during critical periods, regulating synaptic plasticity (Pizzorusso et al., 2002; Gogolla et al., 2009; Mauney et al., 2013). These structures have been the primary focus of studies establishing the importance of CSPGs in adult neural functions. However, evidence for the existence of other ECM structures, such as periaxonal aggregates, has also been reported (Bruckner et al., 2008; Morawski et al., 2010; Lendvai et al., 2012). Periaxonal aggregates were first described by Bruckner et al. who named them "axonal coats" (Bruckner et al., 2008; Morawski et al., 2010). These findings were later reconsidered by these authors, who suggested that in the human lateral geniculate nucleus, these structures may instead correspond to perisynaptic aggregates (Lendvai et al., 2012). However, preliminary observations by our group suggested that, at least in the mediodorsal nucleus of the thalamus (MD), CSPGs do form tubular structures surrounding axons. These preliminary findings prompted further investigations.

Indirect but compelling evidence for the presence of axonal coats comes from a growing body of literature supporting the involvement of the ECM in axonal functions. For example, CSPGs regulate myelination, fasciculation, saltatory impulse conduction, and synaptic functions during development and adulthood. During developmental stages, CSPGs are involved in axonal guidance, including cortico-thalamic axons, and changes in CS sulfation have profound effects on this process (Viapiano and Matthews, 2006; Miyata et al., 2012; Berretta et al., 2015; Fawcett, 2015). Furthermore, several CSPGs play key roles in oligodendrocyte maturation, which in turn impacts myelination of cortico-thalamic axons (Sim et al., 2006; Faissner et al., 2010; Takahashi et al., 2011). During development, glia-derived CSPGs have been shown to regulate axon growth, axon guidance, and axonal fasciculation (Wilson and Snow, 2000; Snow et al., 2003; Ichijo, 2004;

Klausmeyer et al., 2011). Importantly, during late development, CSPGs are key contributors to the powerful inhibition that CNS myelination exerts on neurite outgrowth, thus instating a mature phase of restricted structural plasticity (Dours-Zimmermann et al., 2009; Giger et al., 2010).

In adulthood, CSPGs interact with oligodendrocyte progenitor cells (OPCs), mature oligodendrocytes, and myelinated axons. Plasticity of myelin sheaths during adulthood has been proposed as an ongoing, activity-dependent process important for learning, through which neural circuit activity is fine-tuned in response to environmental experience (McKenzie et al., 2014; Xiao et al., 2016; Hill et al., 2018; Hughes et al., 2018). CSPGs potently regulate OPC differentiation and oligodendrocyte process outgrowth and myelination and are strongly expressed by OPCs themselves (Ichihara-Tanaka et al., 2006; Trotter et al., 2010; Lau et al., 2012). Several CSPGs, including BCAN and NG2, are key components of the nodes of Ranvier, where they regulate axonal conductance (Huang et al., 2005; Melendez-Vasquez et al., 2005; Dours-Zimmermann et al., 2009; Hunanyan et al., 2010). NG2, a CSPG involved in key brain functions such as instructive guidance cues, synaptic plasticity, regulation of the nodes of Ranvier as well as blood-brain-barrier biology, has long been used as a specific OPC marker (Butt et al., 1999; Yang et al., 2006; Kucharova and Stallcup, 2010, 2015; Ferrara et al., 2016; Serwanski et al., 2017). BCAN is secreted by OPCs during active myelination, consistent with its involvement in regulating this process (Bekku and Oohashi, 2010).

Despite their potential broad implications in the regulation of axonal functions, the existence of axonal coats in the adult human brain remains unconfirmed. We tested the hypothesis that BCAN and NG2 form axonal coats, i.e., ECM structures ensheathing axons in the healthy adult human brain. To this end, we focused on the MD, a brain region containing abundant axons, easily identifiable within its pars fasciculata, where they are arranged in large bundles.

MATERIALS AND METHODS

Human Subjects

Tissue blocks containing the whole thalamus from healthy control donors were used for these investigations ($n = 5$ for dual immunofluorescence studies; $n = 3$ for electron microscopy studies) (Table 1). All tissue blocks were obtained from the Harvard Brain Tissue Resource Center (HBTRC), NeuroBioBank site, McLean Hospital, Belmont, MA, United States. Neuropathological assessment of each donor did not show diagnostic findings. The cohort did not include subjects with evidence for gross and/or macroscopic brain changes, or clinical history, consistent with cerebrovascular accidents or other neurological disorders. Subjects with Braak and Braak stages III or higher were not included. Review of extensive clinical records and family questionnaires by HBTRC clinicians ruled out psychiatric disorders. None of the subjects had significant history of substance dependence within 10 or more years from death, as further corroborated by negative toxicology reports. Absence

of recent substance abuse is typical for samples from the HBTRC, which receives exclusively community-based brain tissue donations.

Tissue Processing

Tissue blocks containing the thalamus were dissected from fresh brains and post-fixed in 0.1 M phosphate buffer (PB) containing 4% paraformaldehyde and 0.1 M Na azide at 4°C for 3 weeks, then cryoprotected at 4°C for 3 weeks (30% glycerol, 30% ethylene glycol, and 0.1% Na azide in 0.1 M PB), embedded in agar, and pre-sliced in 2 mm coronal slabs using an Antithetic Tissue Slicer (Stereological Research Lab., Aarhus, Denmark). Each slab was exhaustively sectioned using a freezing microtome (American Optical 860, Buffalo, NY, United States). Sections were stored in cryoprotectant at -20°C. Using systematic random sampling criteria, sections through the thalamus were serially distributed in 26 compartments (40 µm thick sections; 1.04 mm section separation within each compartment). All sections within one compartment/subject were selected for each marker, thus respecting the “equal opportunity” rule (Coggeshall and Lekan, 1996; Gundersen et al., 1999).

Primary Antibodies

NG2 – rabbit polyclonal IgG anti-CSPG4 (55027-1-AP, lot#09000034, Protein Tech Group Inc., Rosemont, IL, United States) raised against a synthetic peptide corresponding to human CSPG4/NG2, GenBank accession # NM_001897.

Brevican – rabbit polyclonal IgG anti-brevican (ab106615, lot#GR163248-6, Abcam, Cambridge, MA, United States), affinity purified, raised against a synthetic peptide corresponding to amino acids 539–588 (PTETLPTPRE RNLASPPST LVEAREVGEA TGGPELSGVP RGESEETGSS) of Human Brevican (NP_940819).

SMI-312 – mouse monoclonal IgG1 anti-SMI312 (ab24574, lot# B226113), Abcam, Cambridge, MA, United States)

recognizing pan-neuronal neurofilaments commonly used as a marker for axons (Ulfing et al., 1998).

Dual Antigen Immunofluorescence

Antigen retrieval was carried out by placing free-floating sections in Vector Antigen Unmasking solution (1:100 in 0.1 M PB; Vector Labs, Burlingame, CA, United States) heated to 80 degrees °C for 1 h. For dual labeling, sections were co-incubated in primary antibodies (NG2, 2 µl:1000 µl, BCAN, 2 µl:1000 µl; SMI-312, 0.5 µl:1000 µl) in 2% bovine serum albumin (BSA) for 72 h at 4°C. This step was followed by 4 h incubation at room temperature in Alexa Fluor goat anti-mouse 594 (1:300 µl; A-11005, Invitrogen, Grand Island, NY, United States) and donkey anti-rabbit 488 (1:300 µl; A-21206, Invitrogen, Grand Island, NY, United States), followed by 10 min in 1 mM CuSO₄ solution (pH 5.0) to block endogenous lipofuscin autofluorescence (Schnell et al., 1999). Sections were mounted and coverslipped using Dako mounting media (S3023, Dako, North America, Carpinteria, CA, United States).

Electron Microscopy: Immunohistochemistry and Tissue Processing

Antigen retrieval was carried out by placing free-floating sections in Vector Antigen Unmasking solution (1:100 in 0.1 M PB; Vector Labs, Burlingame, CA, United States) heated to 80 degrees °C for 1 h. Sections were then rinsed and incubated in 0.05 M glycine (4°C, 1 h, Sigma Millipore) to bind free aldehydes, followed by rinses and blocking in preblocking solution, which contained 10% normal serum of the secondary antibody host animal, Triton-X100 (0.025%, Roche Applied Science; EM), and cold-water fish gelatin (0.1%, Aurion; EM) for stabilization of ultrastructure. Sections were then incubated in primary antibody (NG2, 2 µl:1000 µl or BCAN, 2 µl:1000 µl) for 72 h at 4°C. For

TABLE 1 | Sample demographic and descriptive characteristics of the cohort used for immunohistochemical investigations.

Samples for Immunofluorescence Studies					
Case/age/sex	Cause of death/Inflammation	Brain weight (g)	PMI (hrs)	Hemisphere	Time of Death
93/70/F	Myocardial infarction (A, N)	1245	18.0	R	07:29
05/26/M	Unknown	1250	18.3	R	NA
25/53/F	Cancer (C, N)	1330	24.0	R	08:32
20/74/M	Cardiac Arrest (A, N)	1490	15.8	R	08:41
40/74/F	Cardiac Arrest (A, N)	1100	23.0	L	11:30
Total/mean ± SD 59.4 ± 20.6/3F, 2M		1283 ± 142.3	19.8 ± 3.5	1L/4R	
Samples for Electron Microscopy Studies					
Case/age/sex	Cause of death/Inflammation	Brain weight (g)	PMI (hrs)	Hemisphere	Time of Death
38/95/F	Myocardial infarction (A, N)	1350	07.1	R	14:50
20/74/M	Cardiac Arrest (A, N)	1490	15.8	R	08:41
92/61/M	Cardiac Arrest (A, N)	1100	10.1	R	12:30
Total/mean ± SD 76.7 ± 17.2/1F, 2M		1313 ± 197.5	11.0 ± 4.4	3R	

A, acute, no prolonged agonal period; C, chronic, with agonal period; I, infection/inflammatory condition present at time of death; N, no significant infection/inflammation present at time of death.

control sections, primary antibodies were omitted. Incubation was enhanced by microwaving (2 min at 150 W, 4°C). After primary antibody incubation, sections were incubated in a gold-conjugated secondary antibody (1:50; UltraSmall ImmunoGold F(ab) fragment of goat anti-mouse IgG; catalog #800.266, Aurion; [RRID:AB_2315632]) in a buffer solution (10% normal goat serum, 10% BSA, 0.2% BSA-c, 0.025% Triton X-100 [Roche Applied Science], and 0.1% cold water fish gelatin [Aurion] in 0.1 M PB), followed by silver enhancement of gold particles (90 min, R-GENT SE-EM kit 500.033, Electron Microscopy Sciences, catalog #255213), quenching with 0.1 M PB rinses, and incubation in enhancement solution (Enhancement conditioning solution 10 × 500.055, Electron Microscopy Sciences, catalog #25830). Sections were photographed using a temporary 0.1 M PB mount on an unsubbed glass slide before the remainder of EM processing. We performed microwave postfixation (6% glutaraldehyde, 2% PFA in 0.1 M PB, 150 W, 15°C) until sample temperatures reached 30–35°C, then left the sections in the fixative to come to room temperature for 30 min, which was followed by 0.1 M PB rinses.

Sections were processed for EM using a protocol optimized for scanning/transmission EM and high-throughput block-face imaging, as described previously (García-Cabezas et al., 2016; Zikopoulos et al., 2018; Liu et al., 2020). Briefly, we postfixated tissue sections for 36 min in 2% osmium tetroxide (Electron Microscopy Sciences) with 1.5% potassium ferrocyanide in 0.1 M PB under vacuum with an initial microwave session (100 W at 4°C, 6 min). After three dH₂O rinses, we incubated the tissue sections for 30 min in 1% thiocarbohydrazide in dH₂O (Sigma Millipore), followed by another three dH₂O rinses. We then incubated tissue sections in a second osmium solution (2% osmium tetroxide in dH₂O), under vacuum, with an initial microwave session (100 W at 4°C, 6 min), for a total of 36 min. Sections were rinsed in three dH₂O rinses and stained overnight at 4°C in 1% uranyl acetate (Electron Microscopy Sciences) in dH₂O. The next day, we rinsed the sections with dH₂O 3 times, and then incubated them in lead aspartate solution (0.066 g lead nitrate, Electron Microscopy Sciences, in 10 ml of 0.4% L-aspartic acid in dH₂O, titrated to pH 5.5 using 20% potassium hydroxide solution, Sigma Millipore) for 30 min at 60°C. We then dehydrated the sections in ascending graded ethanol solutions (50, 75, 85, 95, and 100%, 3 min × 5 min each). Sections were then infiltrated with propylene oxide (2 min × 10 min, Electron Microscopy Sciences), followed by a 1:1 mixture of LX112 resin (LX112 Embedding Kits, Ladd Research Industries) and propylene oxide for 1 h, and finally with a 2:1 mixture of LX112 and propylene oxide at 25°C overnight. The following day, the sections were infiltrated with pure LX112 resin for 4 h under vacuum, and then flat embedded in LX112 resin between sheets of Aclar (Ted Pella), and cured for at least 48 h at 60°C. Using a stereoscope, we dissected small cubes of Aclar-embedded tissue, using the photographs of each section taken before EM processing to identify fiducial landmarks (e.g., blood vessels) and precisely locate our regions of interest, and prepared LX112 resin blocks. These blocks were then cured for ≥48 h at 60°C. For block-face imaging, aluminum pins containing cubes of tissue were prepared using conductive epoxy glue (Chemtronics,

catalog #CW2400). We used an ultramicrotome (Ultracut UCT, Leica Microsystems) to expose the surface of the tissue in resin blocks and pins. After exposing the tissue, pins for block-imaging were painted with conductive silver paint (Ted Pella, catalog #16035), which reduces charging artifacts in the scanning electron microscope (SEM). After the tissue was exposed on the resin blocks for the TEM, we cut ~50 nm ultrathin sections and collected them sequentially on pioloform-coated copper slot grids to form a series of 20–300 sections.

Data Collection

Dual-Immunofluorescence Confocal Microscopy Quantification

A Zeiss Axio Imager M2 with a Lumencor SOLA LED lamp interfaced with StereoInvestigator 10.0 (MicroBrightfield Inc., Williston, VT, United States) was used for analysis. The borders of the MD thalamus were delineated using a 1.6× objective according to cytoarchitectonic and myeloarchitectonic criteria as described by Hirai and Jones (1989). Adjacent Nissl and luxol blue stained sections were used as references for delineation of each immunostained section. One set of 40 μm thick serial sections per subject representing the rostral to caudal extent of the MD thalamus (10–12 sections/subject; 1.04 mm section separation within each set) was used for stereology-based quantification. A sampling grid was randomly placed over the MD on each section using the Stereo-Investigator optical fractionator sampling method in order to obtain counting frame sampling sites in a systematic random sampling manner (Gundersen et al., 1999; Dorph-Petersen et al., 2000).

A pilot study was used to determine the optimal grid and counting frame size. On the basis of this pilot study, we chose a grid size of 800 μm × 800 μm and a counting frame size of 300 μm × 300 μm. Using a 63× oil immersion objective (Zeiss Plan Apochromat No. 440760; numeric aperture 1.4; working distance 0.19 mm), we counted all cross-sectional SMI-312-immunoreactive (IR) axons with or without axonal coats, and all NG2- or BCAN-IR axonal coats within each counting frame. Confocal images obtained using a Leica TCS-SP8 confocal microscope with a 100× oil immersion objective were used for confirmation and for measurements of axonal diameter and axonal coat thickness. High-resolution confocal images were scanned at 1 μm intervals through the extent of the z-axis, resulting in 26–32 scans per image.

Electron Microscopy

Electron microscopy (EM) images were obtained using an 80 kV transmission electron microscope (TEM, 100CX, JEOL) at 2000–26,000×. ROIs were sampled systematically, and images were captured for analysis using a digital camera (DigitalMicrograph, Gatan). EM stacks were aligned manually in Reconstruct (Fiala, 2005). For block-face imaging, pins were mounted into the 3View 2XP System (Gatan) coupled to a 1.5 kV scanning electron microscope (GeminiSEM 300, Carl Zeiss). The surface of the pin was imaged using a backscatter detector at 6.5 nm/pixel resolution. A built-in automated

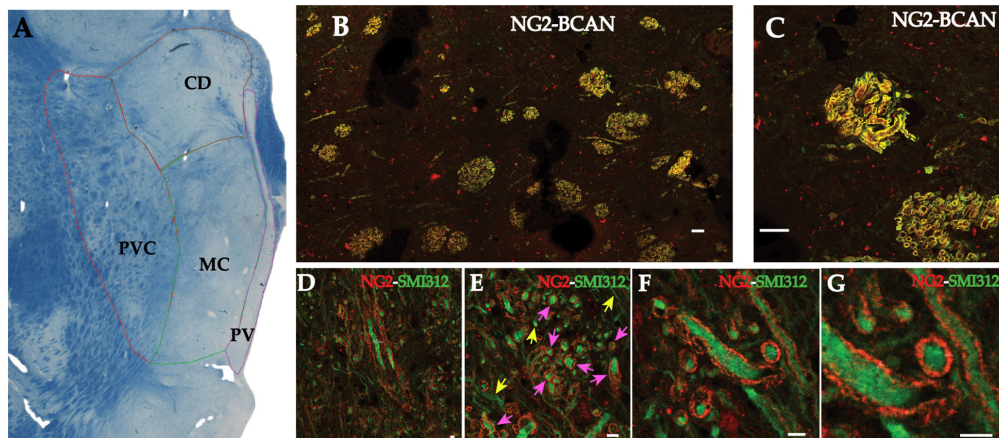


FIGURE 1 | NG2 and BCAN form coats surrounding axons in the human MD thalamus. Photomicrograph of a luxol blue stained section depicting the subregions of the human mediodorsal nucleus sampled for quantification of axonal coats (A). Myelinated fiber bundles were sampled from the parvocellular (PVC), the magnocellular (MC), caudodorsalis (CD) regions of the MD. (B) Low magnification (10×) confocal image of NG2 labeling (red) and BCAN labeling (green) in the mediodorsal nucleus of the human thalamus. Labeling for both CSPGs was observed in structures resembling myelinated fiber bundles. Higher magnification images (C) revealed that these CSPGs labeled tube-like structures apparently surrounding openings that were consistent with the diameters of single axons. Scale bar equals 30 μm . Confocal micrographs of dual immunofluorescence labeling revealed that these CSPG structures resembling axonal coats, labeled with NG2 (red), surrounded SMI-312 immunoreactive axons (green). (D) Low magnification (10× objective) image showing NG2 axonal coats around SMI-312 axons in transverse and cross-section slices of the axons. (E) An intermediate magnification image depicting an example of cross-sectional SMI-312 axons surrounded by NG2 coats. Pink arrows indicate axons surrounded by NG2 coats, yellow arrows indicate axons without NG2 coats. (F) High-resolution imaging allowed for measurements of the diameter of these axons (3.95 and 3.99 μm) as well as the thickness of the NG2 axonal coats [892 and 856 nanometers; (G)]. Scale bars equal 4 μm for D–G.

microtome then cut a 50 nm section from the surface of the pin, and the ROIs were imaged again. This way, long series of ≥ 300 sections were imaged in sequence at each ROI. For series obtained using block-face imaging, we used an algorithm for alignment (GMS3.0, Gatan). EM images and stacks were imported into Reconstruct (Fiala, 2005), where we exhaustively outlined all myelinated axons, identified the distribution of labeling in distinct compartments of the axon, and estimated the major diameter of each axon. Some labeled axons were followed in very long series and reconstructed into 3D models using Reconstruct and Studio Max (Autodesk) for basic smoothing.

RESULTS

NG2 and Brevican Form Tubular Structures Surrounding Axons in the Human Mediodorsal Thalamus

Multiplex immunocytochemistry combined with high-resolution confocal microscopy was used to assess the relationship between SMI-312-IR axons and NG2- and BCAN-IR in the human MD thalamus. NG2- and BCAN-IR were concentrated within axon bundles in the MD (Figure 1A). Within these bundles, NG2- and BCAN-IR were found to co-localize within tube-like structures, resembling myelin sheaths (Figure 1). Dual-labeling with the axonal marker SMI-312 shows that BCAN/NG2-IR tubular structures tightly surround axons (Figure 1). They are referred to here as ‘axonal coats.’ High-resolution confocal microscopy measurements show that the diameter of axonal coats within the

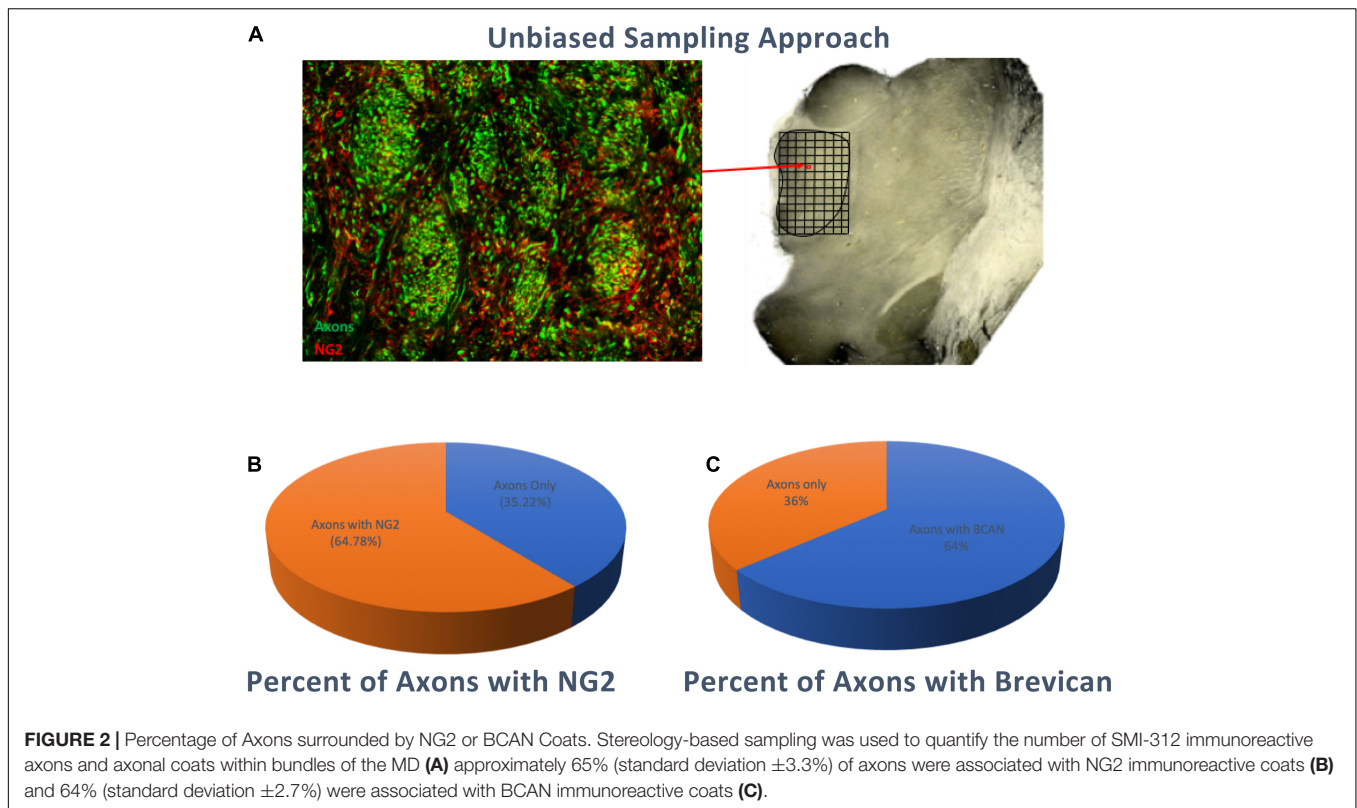
human MD is 3.95–3.99 μm and the thickness of their walls is 856–892 nm (Figures 1E,F).

Axons Within the Human Mediodorsal Thalamic Nucleus Are Predominantly Associated With Axonal Coats

Unbiased stereology-based sampling in 5 control subjects was used to quantify the percentage of axons in the human MD surrounded by NG2-IR and BCAN-IR axonal coats. Our results show that 64.78% (standard deviation $\pm 3.3\%$) of axons were surrounded by NG2-IR coats and 64% (standard deviation $\pm 2.7\%$) by BCAN-IR coats, consistent with predominant colocalization of these CSPGs. Conversely, 35.22% (standard deviation $\pm 3.3\%$) and 36% (standard deviation $\pm 2.7\%$) of axons were not associated with NG2-IR and BCAN-IR axonal coats, respectively (Figure 2).

Ultrastructural Characteristics of NG2- and Brevican-Immunoreactive Axonal Coats

Electron microscopy analysis of BCAN- and NG2-IR axonal coats in the human MD was carried out on a total of 24,148 cross-sections of axon segments from randomly selected sections. We focused on the location of each CSPG with respect to the axon and its myelin sheath and measured the incidence BCAN- and NG2-IR within the axon cytoplasm, just below the myelin sheath outside the axoplasm, or above the myelin sheath on the surface of the myelinated axon.



Distribution of Axonal Coat Labeling With Respect to Axonal Segments

In randomly selected photomicrographs of sections labeled for BCAN, 17% of the axon segments showed BCAN-IR interleaved between myelin layers or associated with axon membrane, 10% of axon segments had BCAN-IR on the surface of the myelin sheath, and 73% of axon segments had no BCAN expression. In sections immunolabeled for NG2, 15% of axon segments showed NG2-IR interleaved with the myelin layers or associated with the axon membrane, 6% of axon segments had NG2-IR on the surface of the myelin sheath, and 79% of axon segments had no NG2 expression. Note that discrepancies between confocal and electron microscopy regarding the percentages of axons associated with BCAN-IR and NG2-IR are explained by the fact that EM detects axons with diameters below 0.1–0.2 μm , which are below the resolution of optical microscopy. Studies from our group and others have reported that EM detects 30–50% more myelinated axons compared to confocal microscopy (Zikopoulos and Barbas, 2010; Liewald et al., 2014; Wegiel et al., 2018; Zikopoulos et al., 2018).

Axonal Coats Are Associated With Medium- and Large-Size Axonal Coats

We assessed whether the relationship between BCAN- and NG2-IR axonal coats and myelin sheaths varies with axon size (**Figure 3**). BCAN-IR axonal coats were not detectable in myelinated axons with a diameter below 0.63 μm on average. In contrast, medium-size axons (average diameter of 0.76 μm), showed a layer of BCAN-IR surrounding the

myelin sheaths. Larger axons, with an average diameter of 0.9907 μm , predominantly showed BCAN-IR interleaved with myelin lamellae or associated with the axon membrane. A similar pattern was observed for NG2-IR axonal coats. Small myelinated axons, with a diameter of 0.53 μm or smaller, did not display NG2-IR axonal coats. Axons with an average diameter of 0.61 μm , showed NG2-IR surrounding the myelin sheets. In larger axons, with an average diameter 0.70 μm , NG2-IR was interleaved with the myelin sheaths or associated with the axon membrane. These findings indicate that BCAN- and NG2-IR axonal coats are predominantly associated with medium- and large-size axons, and that their spatial relationship with the axon and its myelin sheets varies according to the axon size.

Spatial Relationships Between Axonal Coats, Axons, and Myelin

To further explore the spatial relationship between axonal coats and myelinated axons, we analyzed 231 axon segments whose length could be studied across at least 300 nanometers. BCAN-IR was detected within the cytoplasm in 38% of the time, between the myelin lamellae 33% of the time, and on the surface of the myelin sheaths 29% of the time (**Figures 3, 4**). We then examined longer segments ($> 10 \mu\text{m}$) of four axons in 3D to show the pattern of BCAN-IR with respect to myelinated axons. To do this, we reconstructed each axon electronically ‘transected’ longitudinally to show the location of BCAN-IR (**Figure 4**). The results show a regular pattern of BCAN-IR, weaving from the surface of the myelin coating to the inside of the axon with a period of approximately 2 μm .

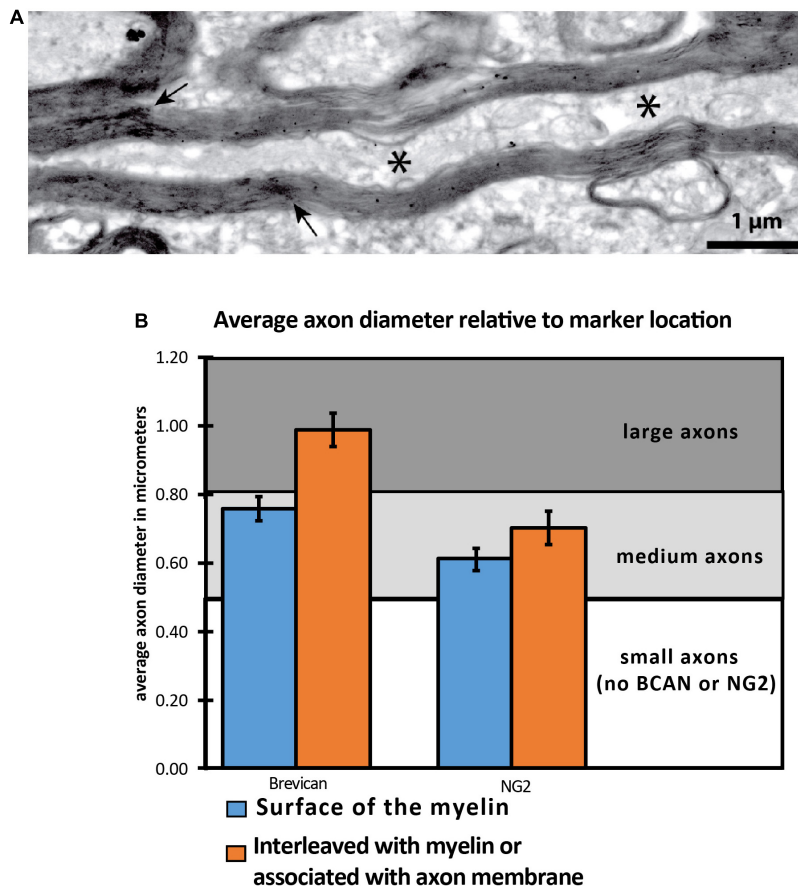


FIGURE 3 | NG2 and BCAN labeling is associated with larger axons. **(A)** Electron microscopy image depicting a cross-sectional axon with myelin labeling and interleaved immunoreactivity for NG2. **(B)** Two-dimensional quantitative analysis of 24,000 axon segments revealed that BCAN and NG2 labeling within the cytoplasm was more frequently observed in larger axons. The * symbol indicates location of the axon.

DISCUSSION

In the human MD, our results show that the CSPGs BCAN and NG2 form tubular sheaths enveloping large- and medium-sized myelinated axons. The term ‘axonal coats,’ originally suggested by Bruckner et al. (2008) and Morawski et al. (2010), aptly describes these ECM/CSPG structures. We describe, to our knowledge for the first time, the ultrastructure of axonal coats, showing that they associate predominantly with medium to large size axons, forming complex structures in relation to myelin sheaths. These findings add to existing evidence for structural relationships between the ECM and neural axons and further point to the involvement of CSPGs in axonal functions. We show that BCAN and NG2 are present not only in the axon initial segment and nodes of Ranvier, where they are thought to regulate neuronal excitability and saltatory conduction, respectively (Butt et al., 1999; John et al., 2006; Bekku et al., 2009; Giger et al., 2010; Hunanyan et al., 2010), but they also surround the axons and interleave with myelin sheaths. In the context of growing support for CSPG functions in the regulation of axon guidance, fasciculation, and myelination, our findings provide evidence for axonal coats as an ECM structure potentially underlying these

functions. Speculatively, given the dynamic role of myelination in the adult brain, where rapid activity-dependent changes in axon myelination support neural plasticity, we put forth the hypothesis that axonal coats may serve to stabilize myelin sheaths in a manner analogous to the role played by PNNs and perisynaptic ECM aggregates in synaptic regulation.

Brevican- and NG2-Immunoreactive Axonal Coats: Association With Medium and Large Axons

NG2- and BCAN-IR axonal coats within the human MD were primarily associated with medium and large axons (Figure 3). This relationship suggests that axonal coats containing these CSPGs may contribute to the high conductance velocity and spike frequencies typical of larger axons, which are mostly involved in long-range pathways (Arbuthnott et al., 1980; Friede et al., 1984; Perge et al., 2009, 2012; Horowitz et al., 2015). Well-established CSPG functions such as regulating ionic homeostasis and providing structural support offer further evidence for this possibility. Interestingly, the predominant association of axonal coats with medium and large axons

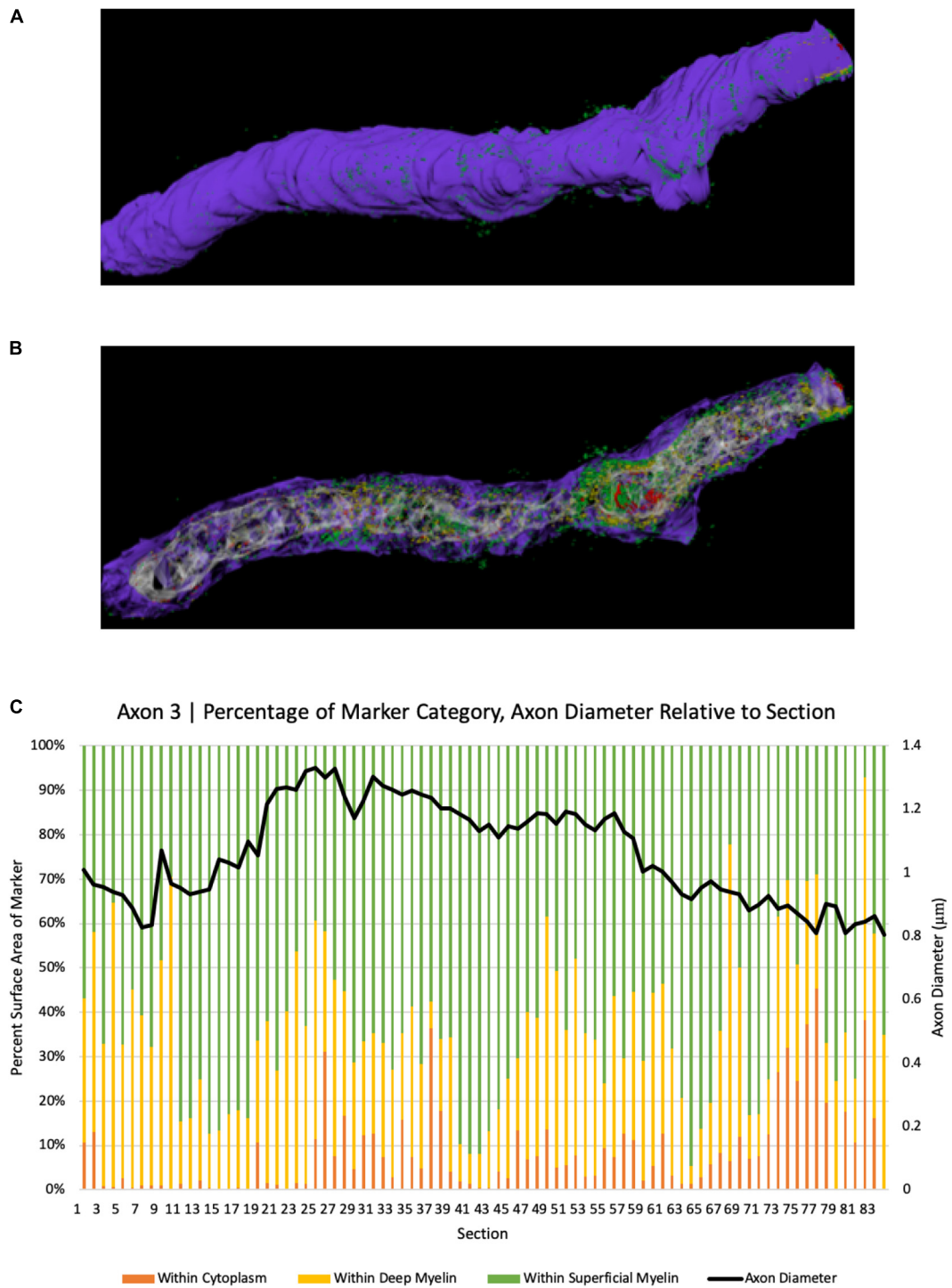


FIGURE 4 | 3D reconstruction of BCAN labeling in a single axon segment. **(A)** Single axonal segment (Axon 3) 11.63 µm long, depicts the outside aspect of the axon. Reconstruction shows the same axon, electronically transected along its longitudinal axis to show the distribution of BCAN in the cytoplasm (red), beneath and between the myelin sheaths **(B)**. **(C)** Quantitative analysis of axon diameter and marker category percentage for each section. Y-axes depict percent surface area of BCAN labeling in each axonal compartment category (left); legend: Purple, myelin; white-gray, cytoplasm; red, within cytoplasm; yellow, marker within deep myelin; green, marker within superficial myelin, and the corresponding axon diameter of each section in microns (right), for each transected axon section analyzed as indicated on the x-axis.

parallels the reported OPC preference to repair minor myelin damage in larger axons (Snaidero et al., 2020; Call and Bergles, 2021).

NG2 is a transmembrane CSPG selectively expressed in the brain OPCs and pericytes (Levine and Card, 1987; Stallcup and Beasley, 1987; Levine et al., 1993; Karram et al., 2008; Moransard et al., 2011; Huang et al., 2014; Stallcup, 2018; Li et al., 2020; Melrose et al., 2021; Chelyshev et al., 2022). OPCs are a major source of mature oligodendrocytes in the adult brain – however, these latter cells are not known to express NG2. Thus, although our study cannot exclude it, it is not likely that the NG2-IR detected in axonal coats is simply a component of the myelin sheaths.

Brevican is secreted into the ECM, where it plays a variety of functional roles, from entering in the composition of PNNs to regulating neuritic functions. The source of BCAN contributing to axonal coats is more difficult to infer, as this CSPG is expressed by neuronal and glial cells, including OPCs (Seidenbecher et al., 2002; John et al., 2006). While BCAN is not expressed by fully mature oligodendrocytes (Ogawa et al., 2001), it is secreted by OPCs during active myelination, consistent with its involvement in regulating this process (Bekku and Oohashi, 2010). Thus, OPCs are also good candidates as a source of BCAN for axonal coats. Notably, evidence supports a key role for BCAN in bridging between the intracellular neuronal domain and the ECM, as it attaches to the surface of the neuronal membrane and interacts with the hyaluronan acid-based extracellular domain (Seidenbecher et al., 2002). This property may be mediated by the adhesion molecule neurofascin 186 kDa isoform (NF-186), which directly links the intracellular cytoskeleton to BCAN-based ECM (Desmazieres et al., 2014). Indeed, interactions between NF-186 and brevican have been found to stabilize the axon initial segment and node of Ranvier (Hedstrom et al., 2007; Kriebel et al., 2012). Speculatively, these observations may account for the axonal coat pattern observed at the ultrastructural level, as BCAN-IR was found to interleave with myelin lamellae as well as associated with the axon.

Ultrastructure of NG2- and Brevican-Axonal Coats

Our ultrastructural analyses showed an intriguing BCAN- and NG2-IR distribution pattern, with a regular wave-like pattern moving from the surface of the myelin sheath, through the myelin layers, within the axon and back to the surface of the myelin sheath (Figure 4). This pattern was more frequently associated with larger axons, suggesting that its functional significance may perhaps be related to structural support. The interleaving pattern formed by axonal coats and myelin lamellae showed a striking regularity, with a period of 2 μm , suggesting a tightly regulated geometric relationship between these structures (Figure 4). Such a short, 2 μm , period is not compatible with the possibility that sites where the axonal coats associate with the axon may correspond to the nodes of Ranvier. This is because the distance between two nodes is expected to be greater, reported to be between 27 and 154 μm at least in the mouse

cortex (Chong et al., 2012; Tomassy et al., 2014; Arancibia-Carcamo et al., 2017). Furthermore, the myelin sheath is clearly visible above the sites where BCAN- and NG2-IR are within or on the surface of the axonal membrane (Figure 4). We put forward the hypothesis that, in larger axons, the interleaving pattern formed by axonal coats and myelin sheaths may help to anchor and stabilize these latter with respect to the axonal cytoskeleton. Speculatively, this function may be analogous to the role played by PNNs and perisynaptic ECM aggregates around active synapses (Faissner et al., 2010; Frischknecht et al., 2014; Ferrer-Ferrer and Dityatev, 2018). Growing evidence for a dynamic, activity-dependent role of myelination, shown to represent a critical aspect of plasticity, is consistent with this hypothesis (McKenzie et al., 2014; Xiao et al., 2016; Hill et al., 2018; Hughes et al., 2018).

Axonal Plasticity and Axonal Conductance

Myelin sheath plasticity occurs throughout adulthood to fine-tune neural circuit activity in response to environmental experience (McKenzie et al., 2014; Xiao et al., 2016; Hill et al., 2018; Hughes et al., 2018). Several lines of evidence suggest that axonal coats may contribute to this process. During late development, CSPGs are key contributors to the powerful inhibition that CNS myelination exerts on neurite outgrowth, thus instating a mature phase of restricted structural plasticity (Dours-Zimmermann et al., 2009; Giger et al., 2010). Furthermore, several studies in rodents suggest that NG2-OPCs contribute to axonal plasticity. For example, sensory deprivation, either *via* whisker trimming or ocular deprivation, causes changes in the number and distribution of NG2-OPCs in these regions, and is associated with altered axonal conductance (Mangin et al., 2012; Etxeberria et al., 2016).

Several CSPGs, including BCAN and NG2, are key components of the nodes of Ranvier. In particular, BCAN has been shown to play a role in determining the specialization and composition of the ECM nodal matrix, particularly in large diameter axons (Bekku et al., 2009). It is tempting to speculate that there may be structural and functional relationships between BCAN/NG2-IR axonal coats and these CSPGs within the nodes of Ranvier. Although it is beyond the scope of the present study, future investigations may assess such relationships and the potential continuity between axonal coats and peri-nodal ECM.

Axon Fasciculation

In the developing brain, CSPGs have been proposed to form axon guidance pathways for thalamocortical axons (Bicknese et al., 1994; Anderson et al., 1998). This function, related to the CSPG inhibitory properties, has been proposed to be a key aspect of axonal fasciculation (Bicknese et al., 1994; Snow et al., 2003). In particular, NG2 and BCAN were reported to have inhibitory effects on axonal growth (Davies et al., 2004; Tan et al., 2005), supporting the hypothesis that BCAN- and NG2-IR axonal coats may contribute to axon fasciculation. This possibility may be particularly relevant in the context of our study, which was focused on large axon bundles within the

MD. Our findings suggest that the large percentage of axonal coats detected in myelinated fiber bundles within the MD may be related to their role in axon fasciculation, promoting the adherence of axons into segregated fiber bundles. It is possible that the high density of large, myelinated fiber bundles in the MD, with a substantial representation of axonal coats, may account for discrepancies between our findings and those reported in the human lateral geniculate nucleus by Lendvai et al. (2012).

Implications for Brain Disorders

Several lines of evidence point to a CSPG dysregulation in a growing number of brain disorders. We previously identified abnormal CSPG expression in the amygdala, entorhinal cortex, prefrontal cortex, and thalamic reticular nucleus of subjects with schizophrenia (Pantazopoulos et al., 2010, 2015; Mauney et al., 2013; Steullet et al., 2018). Our group has also reported widespread ECM abnormalities involving genes encoding for CSPGs, matrix metalloproteases, link proteins, and semaphorins in several cortical and subcortical brain regions (Pantazopoulos et al., 2021). Recent genetic studies, including GWAS, have reported associations of genetic polymorphisms for genes encoding specific CSPGs, such as neurocan, neuroglycan-C, and PTPRZ1, and molecules involved in the regulation of CSPGs including matrix metalloproteases (Buxbaum et al., 2008; Dow et al., 2011; Ripke and Consortium, 2011; Bespalova et al., 2012; Muhleisen et al., 2012; McGrath et al., 2013; Consortium, 2014; Ripke and Schizophrenia Working Group of the Psychiatric Genomics, 2014), suggesting that CSPG abnormalities represent core aspects of the neuropathophysiology of schizophrenia. NG2 has been implicated in this disorder in at least one study (de Vrij et al., 2019).

Extensive evidence from functional imaging studies has identified disrupted cortico-thalamic functional connectivity in subjects with schizophrenia (Schlosser et al., 2003a,b; Marengo et al., 2012; Anticevic et al., 2014; Saalman, 2014; Canu et al., 2015; Cho et al., 2015; Hoflich et al., 2015; Lui et al., 2015). Impaired connectivity of this pathway is believed to impact several clinical aspects of this disorder, including psychosis, attention sensory motor integration, and emotional processing. DTI/fiber tractography studies in subjects with schizophrenia provide strong evidence for a disruption of anatomical connectivity and white matter integrity between cortical areas and thalamus (Rose et al., 2006; Kim et al., 2008; Kito et al., 2009; Oh et al., 2009; Antonius et al., 2011; Sui et al., 2011; Kubota et al., 2012; Marengo et al., 2012). Furthermore, evidence for myelination deficits comes from reports of altered expression of myelin-related proteins and modest oligodendrocyte reduction in the MD and other thalamic nuclei (Schmitt et al., 2004; Byne et al., 2006, 2008; Beasley et al., 2009; Martins-de-Souza et al., 2010). In this context, deficits in axonal coats composed of CSPGs from OPCs may contribute to thalamo-cortical dysconnectivity in schizophrenia.

White matter and oligodendrocyte pathology have also been reported in Alzheimer's disease and proposed to precede disease symptoms (Lee et al., 2016, 2018; Araque Caballero et al., 2018; Nasrabady et al., 2018). Recent studies support a role for CSPG

abnormalities in Alzheimer's disease, including PNN deficits, CSPG expression in amyloid beta plaques, decreased CSF levels of NG2, and increased levels of chondroitin-4-sulfate (Bruckner et al., 1999; Baig et al., 2005; Morawski et al., 2010; Lendvai et al., 2013; Nielsen et al., 2013, 2014; Vegh et al., 2014; Howell et al., 2015; Yang et al., 2017; Cattaud et al., 2018; Schultz et al., 2018). Potential decreases of axonal coats may therefore contribute to white matter connectivity deficits in these diseases.

CONCLUSION

In summary, our data support the existence of a novel ECM structure, axonal coats, in the human MD thalamus, composed of the CSPGs NG2 and BCAN, interweaved between myelin sheaths and axonal plasma membranes. CSPG axonal coats may contribute to several aspects of axon regulation, including fasciculation, axonal guidance, and stabilization of myelin sheath. CSPG involvement in several brain disorders, including schizophrenia and Alzheimer's disease, raises the possibility that axonal coat abnormalities may contribute to connectivity dysfunction reported in these disorders.

DATA AVAILABILITY STATEMENT

The data that support the findings of this study are available from the authors upon reasonable request.

ETHICS STATEMENT

Postmortem human brain samples included in this study were obtained from the Harvard Brain Tissue Resource Center (HBTRC), an NIH NeuroBioBank site. HBTRC protocols for collection and distribution of human brain specimens for research purposes were reviewed and approved by the Mass General Brigham Institutional Review Board. Written informed consent for brain recovery and use for research was provided by the donors' legal next of kin/legal representative.

AUTHOR CONTRIBUTIONS

All authors listed have made a substantial, direct, and intellectual contribution to the, work, and approved it for publication.

FUNDING

This work was funded by NIMH R01 MH105608.

ACKNOWLEDGMENTS

The authors would like to thank the NIH NeuroBioBank, Harvard Brain Tissue Resource Center site, as well as brain donors and their families for the tissue samples used in these studies.

REFERENCES

- Anderson, R. B., Walz, A., Holt, C. E., and Key, B. (1998). Chondroitin sulfates modulate axon guidance in embryonic *Xenopus* brain. *Dev. Biol.* 202, 235–243. doi: 10.1006/dbio.1998.9006
- Anticevic, A., Cole, M. W., Repovs, G., Murray, J. D., Brumbaugh, M. S., Winkler, A. M., et al. (2014). Characterizing thalamo-cortical disturbances in schizophrenia and bipolar illness. *Cereb. Cortex* 24, 3116–3130. doi: 10.1093/cercor/bht165
- Antonius, D., Prudent, V., Rebani, Y., D'Angelo, D., Ardekani, B. A., Malaspina, D., et al. (2011). White matter integrity and lack of insight in schizophrenia and schizoaffective disorder. *Schizophr. Res.* 128, 76–82. doi: 10.1016/j.schres.2011.02.020
- Arancia-Carcamo, I. L., Ford, M. C., Cossell, L., Ishida, K., Tohyama, K., and Attwell, D. (2017). Node of Ranvier length as a potential regulator of myelinated axon conduction speed. *eLife* 6:e23329. doi: 10.7554/eLife.23329
- Araque Caballero, M. A., Suarez-Calvet, M., Duering, M., Franzmeier, N., Benzinger, T., Fagan, A. M., et al. (2018). White matter diffusion alterations precede symptom onset in autosomal dominant Alzheimer's disease. *Brain* 141, 3065–3080. doi: 10.1093/brain/awy229
- Arbuthnot, E. R., Boyd, I. A., and Kalu, K. U. (1980). Ultrastructural dimensions of myelinated peripheral nerve fibres in the cat and their relation to conduction velocity. *J. Physiol.* 308, 125–157. doi: 10.1113/jphysiol.1980.sp013465
- Baig, S., Wilcock, G. K., and Love, S. (2005). Loss of perineuronal net N-acetylgalactosamine in Alzheimer's disease. *Acta Neuropathol.* 110, 393–401. doi: 10.1007/s00401-005-1060-2
- Bandtlow, C. E., and Zimmermann, D. R. (2000). Proteoglycans in the developing brain: new conceptual insights for old proteins. *Physiol. Rev.* 80, 1267–1290. doi: 10.1152/physrev.2000.80.4.1267
- Beasley, C. L., Dwork, A. J., Rosoklija, G., Mann, J. J., Mancevski, B., Jakovski, Z., et al. (2009). Metabolic abnormalities in fronto-striatal-thalamic white matter tracts in schizophrenia. *Schizophr. Res.* 109, 159–166. doi: 10.1016/j.schres.2009.01.017
- Bekku, Y., and Oohashi, T. (2010). Neurocan contributes to the molecular heterogeneity of the perinodal ECM. *Arch. Histol. Cytol.* 73, 95–102. doi: 10.1679/aohc.73.95
- Bekku, Y., Rauch, U., Ninomiya, Y., and Oohashi, T. (2009). Brevican distinctively assembles extracellular components at the large diameter nodes of Ranvier in the CNS. *J. Neurochem.* 108, 1266–1276. doi: 10.1111/j.1471-4159.2009.05873.x
- Berretta, S., Pantazopoulos, H., Markota, M., Brown, C., and Batzianouli, E. T. (2015). Losing the sugar coating: potential impact of perineuronal net abnormalities on interneurons in schizophrenia**. *Schizophr. Res.* 167, 18–27. doi: 10.1016/j.schres.2014.12.040
- Bespalova, I. N., Angelo, G. W., Ritter, B. P., Hunter, J., Reyes-Rabanillo, M. L., Siever, L. J., et al. (2012). Genetic variations in the ADAMTS12 gene are associated with schizophrenia in Puerto Rican patients of Spanish descent. *Neuromolecular Med.* 14, 53–64. doi: 10.1007/s12017-012-8169-y
- Bicknese, A. R., Sheppard, A. M., O'Leary, D. D., and Pearlman, A. L. (1994). Thalamocortical axons extend along a chondroitin sulfate proteoglycan-enriched pathway coincident with the neocortical subplate and distinct from the efferent path. *J. Neurosci.* 14, 3500–3510. doi: 10.1523/JNEUROSCI.14-06-03500.1994
- Bruckner, G., Hausen, D., Hartig, W., Drlicek, M., Arendt, T., and Brauer, K. (1999). Cortical areas abundant in extracellular matrix chondroitin sulphate proteoglycans are less affected by cytoskeletal changes in Alzheimer's disease. *Neuroscience* 92, 791–805. doi: 10.1016/s0306-4522(99)00071-8
- Bruckner, G., Morawski, M., and Arendt, T. (2008). Aggrecan-based extracellular matrix is an integral part of the human basal ganglia circuit. *Neuroscience* 151, 489–504. doi: 10.1016/j.neuroscience.2007.10.033
- Butt, A. M., Duncan, A., Hornby, M. F., Kirvell, S. L., Hunter, A., Levine, J. M., et al. (1999). Cells expressing the NG2 antigen contact nodes of Ranvier in adult CNS white matter. *Glia* 26, 84–91.
- Buxbaum, J. D., Georgieva, L., Young, J. J., Plescia, C., Kajiwara, Y., Jiang, Y., et al. (2008). Molecular dissection of NRG1-ERBB4 signaling implicates PTPRZ1 as a potential schizophrenia susceptibility gene. *Mol. Psychiatry* 13, 162–172. doi: 10.1038/sj.mp.4001991
- Byne, W., Dracheva, S., Chin, B., Schmeidler, J. M., Davis, K. L., and Haroutunian, V. (2008). Schizophrenia and sex associated differences in the expression of neuronal and oligodendrocyte-specific genes in individual thalamic nuclei. *Schizophr. Res.* 98, 118–128. doi: 10.1016/j.schres.2007.09.034
- Byne, W., Kidkardnee, S., Tatusov, A., Yiannoulos, G., Buchsbaum, M. S., and Haroutunian, V. (2006). Schizophrenia-associated reduction of neuronal and oligodendrocyte numbers in the anterior principal thalamic nucleus. *Schizophr. Res.* 85, 245–253. doi: 10.1016/j.schres.2006.03.029
- Call, C. L., and Bergles, D. E. (2021). Cortical neurons exhibit diverse myelination patterns that scale between mouse brain regions and regenerate after demyelination. *Nat. Commun.* 12, 4767. doi: 10.1038/s41467-021-25035-2
- Canu, E., Agosta, F., and Filippi, M. (2015). A selective review of structural connectivity abnormalities of schizophrenic patients at different stages of the disease. *Schizophr. Res.* 161, 19–28. doi: 10.1016/j.schres.2014.05.020
- Cattaud, V., Bezzina, C., Rey, C. C., Lejards, C., Dahan, L., and Verret, L. (2018). Early disruption of parvalbumin expression and perineuronal nets in the hippocampus of the Tg2576 mouse model of Alzheimer's disease can be rescued by enriched environment. *Neurobiol. Aging* 72, 147–158. doi: 10.1016/j.neurobiolaging.2018.08.024
- Celio, M. R., Spreafico, R., De Biasi, S., and Vitellaro-Zuccarello, L. (1998). Perineuronal nets: past and present. *Trends Neurosci.* 21, 510–515. doi: 10.1016/s0166-2236(98)01298-3
- Charvet, I., Hemming, F. J., Feuerstein, C., and Saxod, R. (1998). Mosaic distribution of chondroitin and keratan sulphate in the developing rat striatum: possible involvement of proteoglycans in the organization of the nigrostriatal system. *Brain Res. Dev. Brain Res.* 109, 229–244. doi: 10.1016/s0165-3806(98)00088-1
- Chelyshev, Y. A., Kabdesh, I. M., and Mukhamedshina, Y. O. (2022). Extracellular Matrix in Neural Plasticity and Regeneration. *Cell. Mol. Neurobiol.* 42, 647–664. doi: 10.1007/s10571-020-00986-0
- Cho, K. I., Shenton, M. E., Kubicki, M., Jung, W. H., Lee, T. Y., Yun, J. Y., et al. (2015). Altered Thalamo-Cortical White Matter Connectivity: Probabilistic Tractography Study in Clinical-High Risk for Psychosis and First-Episode Psychosis. *Schizophr. Bull.* 42, 723–31. doi: 10.1093/schbul/sbv169
- Chong, S. Y., Rosenberg, S. S., Fancy, S. P., Zhao, C., Shen, Y. A., Hahn, A. T., et al. (2012). Neurite outgrowth inhibitor Nogo-A establishes spatial segregation and extent of oligodendrocyte myelination. *Proc. Natl. Acad. Sci. U.S.A.* 109, 1299–1304. doi: 10.1073/pnas.1113540109
- Cichon, S., Muhleisen, T. W., Degenhardt, F. A., Mattheisen, M., Miro, X., Strohmaier, J., et al. (2011). Genome-wide association study identifies genetic variation in neurocan as a susceptibility factor for bipolar disorder. *Am. J. Hum. Genet.* 88, 372–381. doi: 10.1016/j.ajhg.2011.01.017
- Coggeshall, R. E., and Lekan, H. A. (1996). Methods for determining number of cells and synapses: a case for more uniform standard of review. *J. Comp. Neurol.* 364, 6–15. doi: 10.1002/(SICI)1096-9861(19960101)364:1<6::AID-CNE2>3.0.CO;2-9
- Consortium, S. W. G. O. T. P. G. (2014). Biological insights from 108 schizophrenia-associated genetic loci. *Nature* 511, 421–427. doi: 10.1038/nature13595
- Davies, J. E., Tang, X., Denning, J. W., Archibald, S. J., and Davies, S. J. (2004). Decorin suppresses neurocan, brevican, phosphacan and NG2 expression and promotes axon growth across adult rat spinal cord injuries. *Eur. J. Neurosci.* 19, 1226–1242. doi: 10.1111/j.1460-9568.2004.03184.x
- de Vrij, F. M., Bouwkamp, C. G., Gunhanlar, N., Shpak, G., Lendemeijer, B., Baghdadi, M., et al. (2019). Candidate CSPG4 mutations and induced pluripotent stem cell modeling implicate oligodendrocyte progenitor cell dysfunction in familial schizophrenia. *Mol. Psychiatry* 24, 757–771. doi: 10.1038/s41380-017-0004-2
- Desmazieres, A., Zonta, B., Zhang, A., Wu, L. M., Sherman, D. L., and Brophy, P. J. (2014). Differential stability of PNS and CNS nodal complexes when neuronal neurofascin is lost. *J. Neurosci.* 34, 5083–5088. doi: 10.1523/JNEUROSCI.4662-13.2014
- Dityatev, A., Frischknecht, R., and Seidenbecher, C. I. (2006). Extracellular matrix and synaptic functions. *Results Probl. Cell Differ.* 43, 69–97.
- Dorph-Petersen, K. A., Gundersen, H. J., and Jensen, E. B. (2000). Non-uniform systematic sampling in stereology. *J. Microsci.* 200, 148–157.
- Dours-Zimmermann, M. T., Maurer, K., Rauch, U., Stoffel, W., Fassler, R., and Zimmermann, D. R. (2009). Versican V2 assembles the extracellular matrix surrounding the nodes of ranvier in the CNS. *J. Neurosci.* 29, 7731–7742. doi: 10.1523/jneurosci.4158-08.2009

- Dow, D. J., Huxley-Jones, J., Hall, J. M., Francks, C., Maycox, P. R., Kew, J. N., et al. (2011). ADAMTS13 as a candidate gene for schizophrenia: gene sequencing and ultra-high density association analysis by imputation. *Schizophr. Res.* 127, 28–34. doi: 10.1016/j.schres.2010.12.009
- Etxeberria, A., Hokanson, K. C., Dao, D. Q., Mayoral, S. R., Mei, F., Redmond, S. A., et al. (2016). Dynamic Modulation of Myelination in Response to Visual Stimuli Alters Optic Nerve Conduction Velocity. *J. Neurosci.* 36, 6937–6948. doi: 10.1523/JNEUROSCI.0908-16.2016
- Faissner, A., Pyka, M., Geissler, M., Sobik, T., Frischknecht, R., Gundelfinger, E. D., et al. (2010). Contributions of astrocytes to synapse formation and maturation - Potential functions of the perisynaptic extracellular matrix. *Brain Res. Rev.* 63, 26–38. doi: 10.1016/j.brainresrev.2010.01.001
- Fawcett, J. W. (2015). The extracellular matrix in plasticity and regeneration after CNS injury and neurodegenerative disease. *Prog. Brain Res.* 218, 213–226. doi: 10.1016/bs.pbr.2015.02.001
- Ferrara, G., Errede, M., Girolamo, F., Morando, S., Ivaldi, F., Panini, N., et al. (2016). NG2, a common denominator for neuroinflammation, blood-brain barrier alteration, and oligodendrocyte precursor response in EAE, plays a role in dendritic cell activation. *Acta Neuropathol.* 132, 23–42. doi: 10.1007/s00401-016-1563-z
- Ferrer-Ferrer, M., and Dityatev, A. (2018). Shaping Synapses by the Neural Extracellular Matrix. *Front. Neuroanat.* 12:40. doi: 10.3389/fnana.2018.00040
- Fiala, J. C. (2005). Reconstruct: a free editor for serial section microscopy. *J. Microsc.* 218, 52–61. doi: 10.1111/j.1365-2818.2005.01466.x
- Friede, R. L., Benda, M., Dewitz, A., and Stoll, P. (1984). Relations between axon length and axon caliber. "Is maximum conduction velocity the factor controlling the evolution of nerve structure"? *J. Neurol. Sci.* 63, 369–380. doi: 10.1016/0022-510x(84)90160-6
- Frischknecht, R., Chang, K. J., Rasband, M. N., and Seidenbecher, C. I. (2014). Neural ECM molecules in axonal and synaptic homeostatic plasticity. *Prog. Brain Res.* 214, 81–100. doi: 10.1016/B978-0-444-63486-3.00004-9
- Frischknecht, R., and Gundelfinger, E. D. (2012). The brain's extracellular matrix and its role in synaptic plasticity. *Adv. Exp. Med. Biol.* 970, 153–171. doi: 10.1007/978-3-7091-0932-8_7
- Garcia-Cabezas, M. A., John, Y. J., Barbas, H., and Zikopoulos, B. (2016). Distinction of Neurons, Glia and Endothelial Cells in the Cerebral Cortex: An Algorithm Based on Cytological Features. *Front. Neuroanat.* 10:107. doi: 10.3389/fnana.2016.00107
- Giger, R. J., Hollis, E. R. II, and Tuszyński, M. H. (2010). Guidance molecules in axon regeneration. *Cold Spring Harb. Perspect. Biol.* 2:a001867. doi: 10.1101/cshperspect.a001867
- Gogolla, N., Caroni, P., Luthi, A., and Herry, C. (2009). Perineuronal nets protect fear memories from erasure. *Science* 325, 1258–1261. doi: 10.1126/science.1174146
- Golgi, C. (1898). Intorno alla struttura delle cellule nervose. *Boll. Soc. Med. Chir. Pavia* 1, 1–14.
- Gundelfinger, E. D., Frischknecht, R., Choquet, D., and Heine, M. (2010). Converting juvenile into adult plasticity: a role for the brain's extracellular matrix. *Eur. J. Neurosci.* 31, 2156–2165. doi: 10.1111/j.1460-9568.2010.07253.x
- Gundersen, H. J., Jensen, E. B., Kieu, K., and Nielsen, J. (1999). The efficiency of systematic sampling in stereology—reconsidered. *J. Microsc.* 193, 199–211. doi: 10.1046/j.1365-2818.1999.00457.x
- Hedstrom, K. L., Xu, X., Ogawa, Y., Frischknecht, R., Seidenbecher, C. I., Shrager, P., et al. (2007). Neurofascin assembles a specialized extracellular matrix at the axon initial segment. *J. Cell. Biol.* 178, 875–886. doi: 10.1083/jcb.200705119
- Hill, R. A., Li, A. M., and Grutzendler, J. (2018). Lifelong cortical myelin plasticity and age-related degeneration in the live mammalian brain. *Nat. Neurosci.* 21, 683–695. doi: 10.1038/s41593-018-0120-6
- Hirai, T., and Jones, E. G. (1989). A new parcellation of the human thalamus on the basis of histochemical staining. *Brain Res. Brain Res. Rev.* 14, 1–34. doi: 10.1016/0165-0173(89)90007-6
- Hoflich, A., Hahn, A., Kublbeck, M., Kranz, G. S., Vanicek, T., Windschberger, C., et al. (2015). Ketamine-Induced Modulation of the Thalamo-Cortical Network in Healthy Volunteers As a Model for Schizophrenia. *Int J Neuropsychopharmacol* 18:pyv040 doi: 10.1093/ijnp/pyv040
- Horowitz, A., Barazany, D., Tavor, I., Bernstein, M., Yovel, G., and Assaf, Y. (2015). In vivo correlation between axon diameter and conduction velocity in the human brain. *Brain Struct. Funct.* 220, 1777–1788. doi: 10.1007/s00429-014-0871-0
- Howell, M. D., Bailey, L. A., Cozart, M. A., Gannon, B. M., and Gottschall, P. E. (2015). Hippocampal administration of chondroitinase ABC increases plaque-adjacent synaptic marker and diminishes amyloid burden in aged APP^{sw/PS1dE9} mice. *Acta Neuropathol. Commun.* 3:54. doi: 10.1186/s40478-015-0233-z
- Huang, J. K., Phillips, G. R., Roth, A. D., Pedraza, L., Shan, W., Belkaid, W., et al. (2005). Glial membranes at the node of Ranvier prevent neurite outgrowth. *Science* 310, 1813–1817. doi: 10.1126/science.1118313
- Huang, W., Zhao, N., Bai, X., Karram, K., Trotter, J., Goebbels, S., et al. (2014). Novel NG2-CreERT2 knock-in mice demonstrate heterogeneous differentiation potential of NG2 glia during development. *Glia* 62, 896–913. doi: 10.1002/glia.22648
- Hughes, E. G., Orthmann-Murphy, J. L., Langseth, A. J., and Bergles, D. E. (2018). Myelin remodeling through experience-dependent oligodendrogenesis in the adult somatosensory cortex. *Nat. Neurosci.* 21, 696–706. doi: 10.1038/s41593-018-0121-5
- Hunanyan, A. S., Garcia-Alias, G., Alessi, V., Levine, J. M., Fawcett, J. W., Mendell, L. M., et al. (2010). Role of chondroitin sulfate proteoglycans in axonal conduction in Mammalian spinal cord. *J. Neurosci.* 30, 7761–7769. doi: 10.1523/JNEUROSCI.4659-09.2010
- Ichihara-Tanaka, K., Oohira, A., Rumsby, M., and Muramatsu, T. (2006). Neuroglycan C is a novel midline receptor involved in process elongation of oligodendroglial precursor-like cells. *J. Biol. Chem.* 281, 30857–30864. doi: 10.1074/jbc.M602228200
- Ichijo, H. (2004). Proteoglycans as cues for axonal guidance in formation of retinotectal or retinocollicular projections. *Mol. Neurobiol.* 30, 23–33.
- John, N., Krugel, H., Frischknecht, R., Smalla, K. H., Schultz, C., Kreutz, M. R., et al. (2006). Brevican-containing perineuronal nets of extracellular matrix in dissociated hippocampal primary cultures. *Mol. Cell. Neurosci.* 31, 774–784. doi: 10.1016/j.mcn.2006.01.011
- Karram, K., Goebbels, S., Schwab, M., Jennissen, K., Seifert, G., Steinhauser, C., et al. (2008). NG2-expressing cells in the nervous system revealed by the NG2-EYFP-knockin mouse. *Genesis* 46, 743–757. doi: 10.1002/dvg.20440
- Kim, D. J., Kim, J. J., Park, J. Y., Lee, S. Y., Kim, J., Kim, I. Y., et al. (2008). Quantification of thalamocortical tracts in schizophrenia and probabilistic maps. *Neuroreport* 19, 399–403. doi: 10.1097/WNR.0b013e3282f56634
- Kito, S., Jung, J., Kobayashi, T., and Koga, Y. (2009). Fiber tracking of white matter integrity connecting the mediodorsal nucleus of the thalamus and the prefrontal cortex in schizophrenia: a diffusion tensor imaging study. *Eur. Psychiatry* 24, 269–274. doi: 10.1016/j.eurpsy.2008.12.012
- Klausmeyer, A., Conrad, R., Faissner, A., and Wiese, S. (2011). Influence of glial-derived matrix molecules, especially chondroitin sulfates, on neurite growth and survival of cultured mouse embryonic motoneurons. *J. Neurosci. Res.* 89, 127–141. doi: 10.1002/jnr.22531
- Kriebel, M., Wuchter, J., Trinks, S., and Volkmer, H. (2012). Neurofascin: a switch between neuronal plasticity and stability. *Int. J. Biochem. Cell. Biol.* 44, 694–697. doi: 10.1016/j.biocel.2012.01.012
- Kubota, M., Miyata, J., Sasamoto, A., Sugihara, G., Yoshida, H., Kawada, R., et al. (2012). Thalamocortical Disconnection in the Orbitofrontal Region Associated With Cortical Thinning in Schizophrenia. *Arch Gen Psychiatry* 70, 12–21. doi: 10.1001/archgenpsychiatry.2012.1023
- Kucharova, K., and Stallcup, W. B. (2010). The NG2 proteoglycan promotes oligodendrocyte progenitor proliferation and developmental myelination. *Neuroscience* 166, 185–194. doi: 10.1016/j.neuroscience.2009.12.014
- Kucharova, K., and Stallcup, W. B. (2015). NG2-proteoglycan-dependent contributions of oligodendrocyte progenitors and myeloid cells to myelin damage and repair. *J. Neuroinflammation* 12:161. doi: 10.1186/s12974-015-0385-6
- Kwok, J. C., Yuen, Y. L., Lau, W. K., Zhang, F. X., Fawcett, J. W., Chan, Y. S., et al. (2012). Chondroitin sulfates in the developing rat hindbrain confine commissural projections of vestibular nuclear neurons. *Neural. Dev.* 7:6. doi: 10.1186/1749-8104-7-6
- Lau, L. W., Keough, M. B., Haylock-Jacobs, S., Cua, R., Doring, A., Sloka, S., et al. (2012). Chondroitin sulfate proteoglycans in demyelinated lesions impair remyelination. *Ann. Neurol.* 72, 419–432. doi: 10.1002/ana.23599

- Lee, S., Vihar, F., Zimmerman, M. E., Narkhede, A., Tosto, G., Benzinger, T. L., et al. (2016). White matter hyperintensities are a core feature of Alzheimer's disease: evidence from the dominantly inherited Alzheimer network. *Ann. Neurol.* 79, 929–939. doi: 10.1002/ana.24647
- Lee, S., Zimmerman, M. E., Narkhede, A., Nasrabad, S. E., Tosto, G., Meier, I. B., et al. (2018). White matter hyperintensities and the mediating role of cerebral amyloid angiopathy in dominantly-inherited Alzheimer's disease. *PLoS One* 13:e0195838. doi: 10.1371/journal.pone.0195838
- Lendvai, D., Morawski, M., Bruckner, G., Negyessy, L., Baksa, G., Glasz, T., et al. (2012). Perisynaptic aggrecan-based extracellular matrix coats in the human lateral geniculate body devoid of perineuronal nets. *J. Neurosci. Res.* 90, 376–387. doi: 10.1002/jnr.22761
- Lendvai, D., Morawski, M., Negyessy, L., Gati, G., Jager, C., Baksa, G., et al. (2013). Neurochemical mapping of the human hippocampus reveals perisynaptic matrix around functional synapses in Alzheimer's disease. *Acta Neuropathol.* 125, 215–229. doi: 10.1007/s00401-012-1042-0
- Levine, J. M., and Card, J. P. (1987). Light and electron microscopic localization of a cell surface antigen (NG2) in the rat cerebellum: association with smooth protoplasmic astrocytes. *J. Neurosci.* 7, 2711–2720. doi: 10.1523/JNEUROSCI.07-09-02711.1987
- Levine, J. M., Stinccone, F., and Lee, Y. S. (1993). Development and differentiation of glial precursor cells in the rat cerebellum. *Glia* 7, 307–321. doi: 10.1002/glia.440070406
- Li, R., Zhang, P., Zhang, M., and Yao, Z. (2020). The roles of neuron-NG2 glia synapses in promoting oligodendrocyte development and remyelination. *Cell. Tissue Res.* 381, 43–53. doi: 10.1007/s00441-020-03195-9
- Liewald, D., Miller, R., Logothetis, N., Wagner, H. J., and Schuz, A. (2014). Distribution of axon diameters in cortical white matter: an electron-microscopic study on three human brains and a macaque. *Biol. Cybern.* 108, 541–557. doi: 10.1007/s00422-014-0626-2
- Liu, X., Bautista, J., Liu, E., and Zikopoulos, B. (2020). Imbalance of laminar-specific excitatory and inhibitory circuits of the orbitofrontal cortex in autism. *Mol. Autism.* 11:83. doi: 10.1186/s13229-020-00390-x
- Lui, S., Yao, L., Xiao, Y., Keedy, S. K., Reilly, J. L., Keefe, R. S., et al. (2015). Resting-state brain function in schizophrenia and psychotic bipolar probands and their first-degree relatives. *Psychol. Med.* 45, 97–108. doi: 10.1017/S003329171400110X
- Maeda, N. (2010). Structural variation of chondroitin sulfate and its roles in the central nervous system. *Cent. Nerv. Syst. Agents Med. Chem.* 10, 22–31.
- Mangin, J. M., Li, P., Scafid, J., and Gallo, V. (2012). Experience-dependent regulation of NG2 progenitors in the developing barrel cortex. *Nat. Neurosci.* 15, 1192–1194. doi: 10.1038/nn.3190
- Marengo, S., Stein, J. L., Savostyanova, A. A., Sambataro, F., Tan, H. Y., Goldman, A. L., et al. (2012). Investigation of anatomical thalamo-cortical connectivity and fMRI activation in schizophrenia. *Neuropsychopharmacology* 37, 499–507. doi: 10.1038/npp.2011.215
- Martins-de-Souza, D., Maccarrone, G., Wobrock, T., Zerr, I., Gormanns, P., Reckow, S., et al. (2010). Proteome analysis of the thalamus and cerebrospinal fluid reveals glycolysis dysfunction and potential biomarkers candidates for schizophrenia. *J. Psychiatr. Res.* 44, 1176–1189. doi: 10.1016/j.jpsychires.2010.04.014
- Mauney, S. A., Athanas, K. M., Pantazopoulos, H., Shaskan, N., Passeri, E., Berretta, S., et al. (2013). Developmental pattern of perineuronal nets in the human prefrontal cortex and their deficit in schizophrenia. *Biol. Psychiatry* 74, 427–435. doi: 10.1016/j.biopsych.2013.05.007
- McGrath, L. M., Cornelis, M. C., Lee, P. H., Robinson, E. B., Duncan, L. E., Barnett, J. H., et al. (2013). Genetic predictors of risk and resilience in psychiatric disorders: a cross-disorder genome-wide association study of functional impairment in major depressive disorder, bipolar disorder, and schizophrenia. *Am. J. Med. Genet. B Neuropsychiatr. Genet.* 162, 779–788. doi: 10.1002/ajmg.b.32190
- McKenzie, I. A., Ohayon, D., Li, H., de Faria, J. P., Emery, B., Tohyama, K., et al. (2014). Motor skill learning requires active central myelination. *Science* 346, 318–322. doi: 10.1126/science.1254960
- Melendez-Vasquez, C., Carey, D. J., Zanazzi, G., Reizes, O., Maurel, P., and Salzer, J. L. (2005). Differential expression of proteoglycans at central and peripheral nodes of Ranvier. *Glia* 52, 301–308. doi: 10.1002/glia.20245
- Melrose, J., Hayes, A. J., and Bix, G. (2021). The CNS/PNS Extracellular Matrix Provides Instructive Guidance Cues to Neural Cells and Neuroregulatory Proteins in Neural Development and Repair. *Int. J. Mol. Sci.* 22:5583. doi: 10.3390/ijms22115583
- Miyata, S., Komatsu, Y., Yoshimura, Y., Taya, C., and Kitagawa, H. (2012). Persistent cortical plasticity by upregulation of chondroitin 6-sulfation. *Nat. Neurosci.* 15, 414–22, S1–2. doi: 10.1038/nn.3023
- Moransard, M., Dann, A., Staszewski, O., Fontana, A., Prinz, M., and Suter, T. (2011). NG2 expressed by macrophages and oligodendrocyte precursor cells is dispensable in experimental autoimmune encephalomyelitis. *Brain* 134, 1315–1330. doi: 10.1093/brain/awr070
- Morawski, M., Bruckner, G., Jager, C., Seeger, G., and Arendt, T. (2010). Neurons associated with aggrecan-based perineuronal nets are protected against tau pathology in subcortical regions in Alzheimer's disease. *Neuroscience* 169, 1347–1363. doi: 10.1016/j.neuroscience.2010.05.022
- Muhleisen, T. W., Mattheisen, M., Strohmaier, J., Degenhardt, F., Priebe, L., Schultz, C. C., et al. (2012). Association between schizophrenia and common variation in neurocan (NCAN), a genetic risk factor for bipolar disorder. *Schizophr. Res.* 138, 69–73. doi: 10.1016/j.schres.2012.03.007
- Nasrabad, S. E., Rizvi, B., Goldman, J. E., and Brickman, A. M. (2018). White matter changes in Alzheimer's disease: a focus on myelin and oligodendrocytes. *Acta Neuropathol. Commun.* 6:22. doi: 10.1186/s40478-018-0515-3
- Nielsen, H. M., Ek, D., Avdic, U., Orbjorn, C., Hansson, O., Netherlands Brain, B., et al. (2013). NG2 cells, a new trail for Alzheimer's disease mechanisms? *Acta Neuropathol. Commun.* 1:7. doi: 10.1186/2051-5960-1-7
- Nielsen, H. M., Hall, S., Surova, Y., Nagga, K., Nilsson, C., Londos, E., et al. (2014). Low levels of soluble NG2 in cerebrospinal fluid from patients with dementia with Lewy bodies. *J. Alzheimers Dis.* 40, 343–350. doi: 10.3233/JAD-132246
- Ogawa, T., Hagihara, K., Suzuki, M., and Yamaguchi, Y. (2001). Brevican in the developing hippocampal fimbria: differential expression in myelinating oligodendrocytes and adult astrocytes suggests a dual role for brevican in central nervous system fiber tract development. *J. Comp. Neurol.* 432, 285–295. doi: 10.1002/cne.1103
- Oh, J. S., Kubicki, M., Rosenberger, G., Bouix, S., Levitt, J. J., McCarley, R. W., et al. (2009). Thalamo-frontal white matter alterations in chronic schizophrenia: a quantitative diffusion tractography study. *Hum. Brain Mapp.* 30, 3812–3825. doi: 10.1002/hbm.20809
- Pantazopoulos, H., Katsel, P., Haroutunian, V., Chelini, G., Klengel, T., and Berretta, S. (2021). Molecular signature of extracellular matrix pathology in schizophrenia. *Eur. J. Neurosci.* 53, 3960–3987. doi: 10.1111/ejn.15009
- Pantazopoulos, H., Markota, M., Jaquet, F., Ghosh, D., Wallin, A., Santos, A., et al. (2015). Aggrecan and chondroitin-6-sulfate abnormalities in schizophrenia and bipolar disorder: a postmortem study on the amygdala. *Transl. Psychiatry* 5:e496. doi: 10.1038/tp.2014.128
- Pantazopoulos, H., Woo, T. U., Lim, M. P., Lange, N., and Berretta, S. (2010). Extracellular matrix-glia abnormalities in the amygdala and entorhinal cortex of subjects diagnosed with schizophrenia. *Arch. Gen. Psychiatry* 67, 155–166. doi: 10.1001/archgenpsychiatry.2009.196
- Perge, J. A., Koch, K., Miller, R., Sterling, P., and Balasubramanian, V. (2009). How the optic nerve allocates space, energy capacity, and information. *J. Neurosci.* 29, 7917–7928. doi: 10.1523/JNEUROSCI.5200-08.2009
- Perge, J. A., Niven, J. E., Mugnaini, E., Balasubramanian, V., and Sterling, P. (2012). Why do axons differ in caliber? *J. Neurosci.* 32, 626–638. doi: 10.1523/JNEUROSCI.4254-11.2012
- Pizzorusso, T., Medini, P., Berardi, N., Chierzi, S., Fawcett, J. W., and Maffei, L. (2002). Reactivation of ocular dominance plasticity in the adult visual cortex. *Science* 298, 1248–1251. doi: 10.1126/science.1072699
- Rauch, U. (2004). Extracellular matrix components associated with remodeling processes in brain. *Cell Mol. Life Sci.* 61, 2031–2045. doi: 10.1007/s00018-004-4043-x
- Ripke, S., and Consortium, T. S. P. G.-W. A. S. (2011). Genome-wide association study identifies five new schizophrenia loci. *Nat. Genet.* 43, 969–976. doi: 10.1038/ng.940
- Ripke, S., and Schizophrenia Working Group of the Psychiatric Genomics, C. (2014). Biological insights from 108 schizophrenia-associated genetic loci. *Nature* 511, 421–427.
- Rose, S. E., Chalk, J. B., Janke, A. L., Strudwick, M. W., Windus, L. C., Hannah, D. E., et al. (2006). Evidence of altered prefrontal-thalamic circuitry in

- schizophrenia: an optimized diffusion MRI study. *NeuroImage* 32, 16–22. doi: 10.1016/j.neuroimage.2006.03.003
- Saalmann, Y. B. (2014). Intralaminar and medial thalamic influence on cortical synchrony, information transmission and cognition. *Front. Syst. Neurosci.* 8:83. doi: 10.3389/fnsys.2014.00083
- Schlosser, R., Gesierich, T., Kaufmann, B., Vucurevic, G., Hunsche, S., Gawehn, J., et al. (2003a). Altered effective connectivity during working memory performance in schizophrenia: a study with fMRI and structural equation modeling. *NeuroImage* 19, 751–763. doi: 10.1016/s1053-8119(03)00106-x
- Schlosser, R., Gesierich, T., Kaufmann, B., Vucurevic, G., and Stoeter, P. (2003b). Altered effective connectivity in drug free schizophrenic patients. *Neuroreport* 14, 2233–2237. doi: 10.1097/01.wnr.0000090956.15465.06
- Schmitt, A., Wilczek, K., Blennow, K., Maras, A., Jatzko, A., Petroianu, G., et al. (2004). Altered thalamic membrane phospholipids in schizophrenia: a postmortem study. *Biol. Psychiatry* 56, 41–45. doi: 10.1016/j.biopsych.2004.03.019
- Schnell, S. A., Staines, W. A., and Wessendorf, M. W. (1999). Reduction of lipofuscin-like autofluorescence in fluorescently labeled tissue. *J. Histochem. Cytochem.* 47, 719–730. doi: 10.1177/002215549904700601
- Schultz, N., Brannstrom, K., Byman, E., Moussaud, S., Nielsen, H. M., Netherlands Brain, B., et al. (2018). Amyloid-beta 1-40 is associated with alterations in NG2+ pericyte population ex vivo and in vitro. *Aging Cell* 17:e12728. doi: 10.1111/ace1.12728
- Seidenbecher, C. I., Smalla, K. H., Fischer, N., Gundelfinger, E. D., and Kreutz, M. R. (2002). Brevican isoforms associate with neural membranes. *J. Neurochem.* 83, 738–746. doi: 10.1046/j.1471-4159.2002.01183.x
- Serwanski, D. R., Jukkola, P., and Nishiyama, A. (2017). Heterogeneity of astrocyte and NG2 cell insertion at the node of ranvier. *J. Comp. Neurol.* 525, 535–552. doi: 10.1002/cne.24083
- Sim, F. J., Lang, J. K., Waldau, B., Roy, N. S., Schwartz, T. E., Pilcher, W. H., et al. (2006). Complementary patterns of gene expression by human oligodendrocyte progenitors and their environment predict determinants of progenitor maintenance and differentiation. *Ann. Neurol.* 59, 763–779. doi: 10.1002/ana.20812
- Snaidero, N., Schifferer, M., Mezydlo, A., Zalc, B., Kerschensteiner, M., and Misgeld, T. (2020). Myelin replacement triggered by single-cell demyelination in mouse cortex. *Nat. Commun.* 11:4901. doi: 10.1038/s41467-020-18632-0
- Snow, D. M., Smith, J. D., Cunningham, A. T., McFarlin, J., and Goshorn, E. C. (2003). Neurite elongation on chondroitin sulfate proteoglycans is characterized by axonal fasciculation. *Exp. Neurol.* 182, 310–321. doi: 10.1016/s0014-4886(03)00034-7
- Stallcup, W. B. (2018). The NG2 Proteoglycan in Pericyte Biology. *Adv. Exp. Med. Biol.* 1109, 5–19. doi: 10.1007/978-3-030-02601-1_2
- Stallcup, W. B., and Beasley, L. (1987). Bipotential glial precursor cells of the optic nerve express the NG2 proteoglycan. *J. Neurosci.* 7, 2737–2744. doi: 10.1523/JNEUROSCI.07-09-02737.1987
- Stellet, P., Cabungcal, J. H., Bukhari, S. A., Ardelt, M. I., Pantazopoulos, H., Hamati, F., et al. (2018). The thalamic reticular nucleus in schizophrenia and bipolar disorder: role of parvalbumin-expressing neuron networks and oxidative stress. *Mol. Psychiatry* 23, 2057–2065. doi: 10.1038/mp.2017.230
- Sui, J., Pearson, G., Caprihan, A., Adali, T., Kiehl, K. A., Liu, J., et al. (2011). Discriminating schizophrenia and bipolar disorder by fusing fMRI and DTI in a multimodal CCA+ joint ICA model. *NeuroImage* 57, 839–855. doi: 10.1016/j.neuroimage.2011.05.055
- Sykova, E., and Nicholson, C. (2008). Diffusion in brain extracellular space. *Physiol. Rev.* 88, 1277–1340. doi: 10.1152/physrev.00027.2007
- Takahashi, N., Sakurai, T., Bozdagi-Gunal, O., Dorr, N. P., Moy, J., Krug, L., et al. (2011). Increased expression of receptor phosphotyrosine phosphatase-beta/zeta is associated with molecular, cellular, behavioral and cognitive schizophrenia phenotypes. *Transl. Psychiatry* 1:e8. doi: 10.1038/tp.2011.8
- Tan, A. M., Zhang, W., and Levine, J. M. (2005). NG2: a component of the glial scar that inhibits axon growth. *J. Anat.* 207, 717–725. doi: 10.1111/j.1469-7580.2005.00452.x
- Thorne, R. G., and Nicholson, C. (2006). In vivo diffusion analysis with quantum dots and dextrans predicts the width of brain extracellular space. *Proc. Natl. Acad. Sci. U.S.A.* 103, 5567–5572. doi: 10.1073/pnas.0509425103
- Tomassy, G. S., Berger, D. R., Chen, H. H., Kasthuri, N., Hayworth, K. J., Vercelli, A., et al. (2014). Distinct profiles of myelin distribution along single axons of pyramidal neurons in the neocortex. *Science* 344, 319–324. doi: 10.1126/science.1249766
- Trotter, J., Karram, K., and Nishiyama, A. (2010). NG2 cells: properties, progeny and origin. *Brain Res. Rev.* 63, 72–82. doi: 10.1016/j.brainresrev.2009.12.006
- Ulfing, N., Nickel, J., and Bohl, J. (1998). Monoclonal antibodies SMI 311 and SMI 312 as tools to investigate the maturation of nerve cells and axonal patterns in human fetal brain. *Cell Tissue Res.* 291, 433–443. doi: 10.1007/s004410051013
- Vegh, M. J., Heldring, C. M., Kamphuis, W., Hijazi, S., Timmerman, A. J., Li, K. W., et al. (2014). Reducing hippocampal extracellular matrix reverses early memory deficits in a mouse model of Alzheimer's disease. *Acta Neuropathol. Commun.* 2:76. doi: 10.1186/s40478-014-0076-z
- Viapiano, M. S., and Matthews, R. T. (2006). From barriers to bridges: chondroitin sulfate proteoglycans in neuropathology. *Trends Mol. Med.* 12, 488–496. doi: 10.1016/j.molmed.2006.08.007
- Wang, H., Katagiri, Y., McCann, T. E., Unsworth, E., Goldsmith, P., Yu, Z. X., et al. (2008). Chondroitin-4-sulfation negatively regulates axonal guidance and growth. *J. Cell Sci.* 121, 3083–3091. doi: 10.1242/jcs.032649
- Wegiel, J., Kaczmarek, W., Flory, M., Martinez-Cerdeno, V., Wisniewski, T., Nowicki, K., et al. (2018). Deficit of corpus callosum axons, reduced axon diameter and decreased area are markers of abnormal development of interhemispheric connections in autistic subjects. *Acta Neuropathol. Commun.* 6:143. doi: 10.1186/s40478-018-0645-7
- Wilson, M. T., and Snow, D. M. (2000). Chondroitin sulfate proteoglycan expression pattern in hippocampal development: potential regulation of axon tract formation. *J. Comp. Neurol.* 424, 532–546. doi: 10.1002/1096-9861(20000828)424:3<aid-cne10>3.0.co;2-z
- Xiao, L., Ohayon, D., McKenzie, I. A., Sinclair-Wilson, A., Wright, J. L., Fudge, A. D., et al. (2016). Rapid production of new oligodendrocytes is required in the earliest stages of motor-skill learning. *Nat. Neurosci.* 19, 1210–1217. doi: 10.1038/nn.4351
- Yamaguchi, Y. (2000). Lecticans: organizers of the brain extracellular matrix. *Cell Mol. Life Sci.* 57, 276–289.
- Yang, S., Hilton, S., Alves, J. N., Saksida, L. M., Bussey, T., Matthews, R. T., et al. (2017). Antibody recognizing 4-sulfated chondroitin sulfate proteoglycans restores memory in tauopathy-induced neurodegeneration. *Neurobiol. Aging* 59, 197–209. doi: 10.1016/j.neurobiolaging.2017.08.002
- Yang, Z., Suzuki, R., Daniels, S. B., Brunquell, C. B., Sala, C. J., and Nishiyama, A. (2006). NG2 glial cells provide a favorable substrate for growing axons. *J. Neurosci.* 26, 3829–3839. doi: 10.1523/JNEUROSCI.4247-05.2006
- Zikopoulos, B., and Barbas, H. (2010). Changes in prefrontal axons may disrupt the network in autism. *J. Neurosci.* 30, 14595–14609. doi: 10.1523/JNEUROSCI.2257-10.2010
- Zikopoulos, B., Liu, X., Tepe, J., Trutzer, I., John, Y. J., and Barbas, H. (2018). Opposite development of short- and long-range anterior cingulate pathways in autism. *Acta Neuropathol.* 136, 759–778. doi: 10.1007/s00401-018-1904-1

Conflict of Interest: The authors declare that the research was conducted in the absence of any commercial or financial relationships that could be construed as a potential conflict of interest.

Publisher's Note: All claims expressed in this article are solely those of the authors and do not necessarily represent those of their affiliated organizations, or those of the publisher, the editors and the reviewers. Any product that may be evaluated in this article, or claim that may be made by its manufacturer, is not guaranteed or endorsed by the publisher.

Copyright © 2022 Pantazopoulos, Hossain, Chelini, Durning, Barbas, Zikopoulos and Berretta. This is an open-access article distributed under the terms of the Creative Commons Attribution License (CC BY). The use, distribution or reproduction in other forums is permitted, provided the original author(s) and the copyright owner(s) are credited and that the original publication in this journal is cited, in accordance with accepted academic practice. No use, distribution or reproduction is permitted which does not comply with these terms.